

Optimization of the AA6061-T6 aluminum alloy Burnishing Process by response surface method

Panuwat Thosa^{1*}, Anantachin Khamsupa²

Division of Industrial Technology, Faculty of Industrial Technology, Nakhon Phanom University

panuwat@npu.ac.th

Abstract

The influence of operational constraints, the burnishing procedure was conceived and formulated with the aim of enhancing the finalization of the workpiece, thereby mitigating production time. This investigation aimed to scrutinize the optimization potential of the burnishing process applied to AA6061-T6 aluminum alloy through CNC lathe operations, with a specific focus on its impact on tensile strength. The experimentation sought to identify the optimal parameters for the burnishing process, establishing a rotational speed of 200 revolutions per minute, a feed rate of 0.2571 meters per minute, and a feed depth of 0.09 millimeters. The resultant outcome exhibited a peak tensile strength of 370 megapascals. Subsequent microstructure analysis of the workpiece revealed that diverse factors exerted negligible influence on the structural integrity, particularly on the injection structure.

Keywords: Burnishing process, Aluminum alloy, Response Surface Method

I. INTRODUCTION

Aluminum, a versatile material extensively employed in diverse industrial sectors such as aerospace, automotive, and shipbuilding, possesses exceptional attributes, including lightness, high tensile strength, and resistance to corrosion. These properties render it highly suitable for a broad spectrum of applications. Presently, aluminum is classified into nine distinct types, spanning from grade 1xxx to 9xxx, with each variant being applied in distinct industrial contexts based on its unique characteristics. In the manufacturing of aluminum components for the automotive industry, a variety of processes are deployed, predominantly encompassing cutting methodologies like shearing, peeling, reducing, and drilling for assembly. These manufacturing procedures exert a substantial influence on the ultimate product quality, encompassing considerations such as surface smoothness and component dimensions. For instance, a predominant proportion of aluminum components within the automotive sector undergo shaping through cutting techniques such as shearing, peeling, reducing, and drilling for assembly. These processes invariably impact the surface finish quality during the shaping phase, with critical factors including surface smoothness, component dimensions, and the inherent constraints of the shaping methodology. Furthermore, the ornamentation of composite aluminum poses challenges owing to the material's hardness or the impracticability of modifying the surface through conventional grinding approaches. Achieving the final surface finish necessitates recourse to a burnishing process, wherein variables such as rotational speed, compaction force, and feed rate assume paramount importance. These variables exert a considerable influence on both the surface smoothness and the mechanical properties of composite aluminum alloys, exemplified by Al 7175-T6, as expounded by Ozer, Melika, et al. in their 2023 discourse [1].

Response Surface Methodology (RSM) is a statistical technique that applies mathematics to analyze and solve problems, focusing on the creation of mathematical models to find optimal or

minimal values of independent variables that lead to the highest or lowest response. The use of response surface methodology helps explore the impact of various variables on the selected response systematically, providing structured guidelines driven by data to make the process more efficient. It aids in predicting the effects of changes in suitable independent variables, reducing the need for extensive experimentation. In September 2022 [2], Saffar, Saber, and Hamid Eslami applied statistical techniques and employed the Taguchi method to analyze the surface pressing process of aluminum alloy 5052. The study aimed to identify the optimal parameters of the machine in the manufacturing process. The findings revealed that the suitable condition for smooth surface pressing is a rotation speed of 200 revolutions per minute, a feed rate of 0.5 meters per minute, and a pressing force of 200 Newtons. The average minimum surface roughness obtained was 0.47 micrometers. Additionally, in April 2021 [3], Suriya Prasomthong and Suriya Namkaew reported that the surface pressing process not only improves the characteristics and quality of the workpiece surface but also enhances its resistance to corrosion in the outer surface, contributing to [4-5].

In the research study mentioned above, it was found that the burnishing process can effectively enhance the quality of the surface of workpieces. Therefore, the researchers aim to investigate the appropriate factors in the burnishing process of aluminum alloy grade AA6061-T6 using ceramic balls. The study examines controllable factors such as rotation speed, feed rate, and force applied during the burnishing process to analyze the results and identify optimal conditions for efficient surface burnishing. The researchers hope that this study will be beneficial for both academic research and future industrial applications.

II. METHOD

2.1 Burnishing process

The burnishing procedure constitutes a methodology employed for the amelioration of the surface condition of a given workpiece, thereby effectuating enhanced smoothness and augmenting its mechanical strength attributes. This technique is universally applicable across diverse material types. Its execution involves the utilization of a burnishing tool, typically configured as a roller, exerted upon the workpiece surface with a precision-centric mechanism. The burnishing process imparts surface refinement by modifying the elevation of the workpiece surface, engendering a sleeker and more lustrous appearance without material removal. This outcome is realized through the utilization of a mobile tool, frequently accompanied by a ball or roller endowed with unrestricted rotational movement upon the surface. Consequently, the burnishing process induces plastic deformation within the surface stratum of the material, as elucidated in Figure 1.

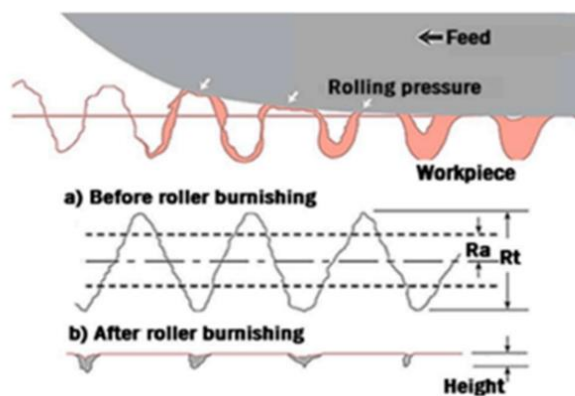


Figure 1. Surface changes by polishing process. [6]

the workpiece is pressed against the rotating surface at a controlled rotational speed and moves forward according to the rate of motion specified by the machine, surface compression is applied to adjust the size and refine the surface of the rapidly moving workpiece. This reduces the time required for the production of machine parts, as the workpiece does not need to be removed from the machine. The entire process can be completed within a single machine, saving time and labor in the manufacturing process. In the automotive industry, the process of surface compression is increasingly being incorporated to enhance production efficiency. This is due to its advantages in accurately controlling the size and quality of the surface, resulting in efficient production of workpiece products. The process simplifies and reduces the cost of production, with minimal deviation, less than 0.0005 inches. The benefits of the surface compression process include.

- Achieve improved surface finish between 1 to 10 microinches Ra.
- Increase workpiece hardness by up to 5 to 10 percent.
- Reduce production cycle time.
- Attain cleaner workpiece surfaces compared to other polishing methods.
- Potential cost savings in the manufacturing process, such as eliminating the need for regrinding or surface burnishing.

the burnishing ball is pressed onto the prepared surface of the workpiece, which has been previously prepared but still exhibits a surface roughness below 80 or retains the original surface (D: Machine Surface), the original surface features a low surface height. When the burnishing ball contacts the surface with an appropriate and constant force during its uniform movement, pressing on the surface results in the flow of material from the wave peaks to the lowest points of the waves on the material's surface. This leads to a uniform and increased surface smoothness, as depicted in point (E: Burnished Surface). Meanwhile, the force applied by the burnishing ball causes permanent deformation (Plastic Deformation) in the material's flow area, creating a compressive residual stress in the surface region that comes into contact. Similarly, the internal surface of the material influenced by the external pressure from the burnishing ball undergoes tensile residual stress, resulting in increased material strength due to the accumulation of external stress. Furthermore, the permanent deformation areas often experience a significant increase in dislocation density, contributing to a higher value of dislocation. Consequently, the dislocation interactions between adjacent surfaces lead to increased surface hardness and strength, with an increase of 5-10 percent or more, as compared to the mechanism of the surface burnishing process, as illustrated in Figure 2.

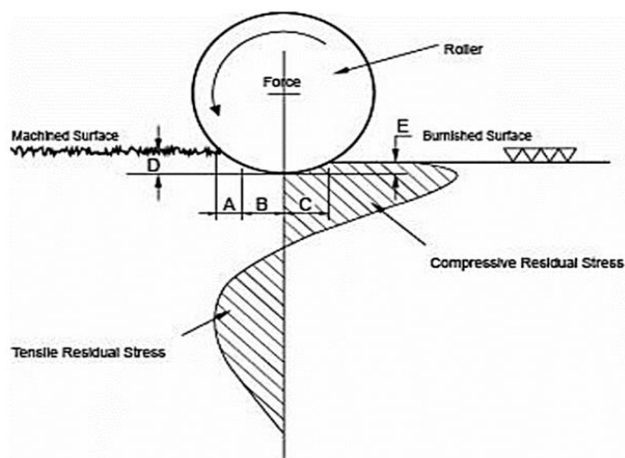


Figure 2. the surface burnishing process.

2.2 Surface burnishing Experiment

the study of factors affecting the performance of machinery in production, experiments on surface burnishing are conducted, including the variables of rotational speed, feed rate, and surface burnishing pressure. All three factors often impact the surface quality of the workpiece [1]. The experiments utilize a CNC lathe machine capable of controlling rotational speed and tool movement with a ceramic ball, maintaining a constant pressure, and a pressing depth of 0.25 millimeters. The pressing is performed in a single operation, and the pressing tool is designed to measure the force applied using a spring as a reference for distance. The adjustable screw mechanism is employed to set the screw pitch, with a force gauge measuring the pressure in surface burnishing. The experimental process is illustrated in Figure 2. Subsequently, the workpiece is measured for surface roughness using a mobile contact measuring tool. The average surface roughness value is then analyzed to assess the efficiency of the experimental process.

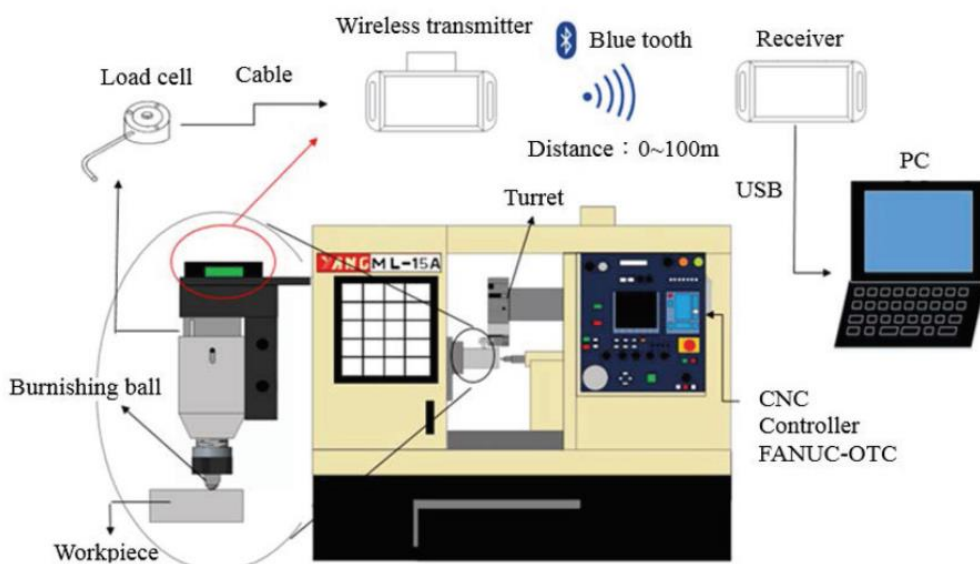


Figure 3. the process of polishing surface of AA6061-T6 aluminum alloy.

2.3 Experimental Design

Response Surface Methodology (RSM) is a technique that integrates mathematical and statistical techniques to model and analyze problems where the response variable is influenced by multiple factors or independent variables. The method is used to construct models and analyze problems related to the response variable, establishing relationships with various factors or independent variables to determine optimal response levels. This experimental design is referred to as Response Surface Design. However, in practical applications, the true nature of the relationship between the response variable and the independent variables is often unknown. Therefore, an approximation of this relationship is necessary, and it is commonly found that a second-order model is preferred. This is because it is less complex and simpler compared to other models while still capable of representing the second-order model as follows.

$$Y = \beta_0 + \sum_{i=1}^3 \beta_i X_i + \sum_{i=1}^3 \beta_{ii} X_i^2 + \sum_{i=1}^2 \sum_{j=i+1}^3 \beta_{ij} X_i X_j \quad (1)$$

Where: y = Response Variable
 x_i = Factor i ; i
 k = Total number of factors

$$\beta_0 = y \text{ intercept}$$

2.4 Experimental Materials

The experimental materials utilized in the study included AA6061-T6 alloy aluminum with a central diameter of 22 millimeters and a length of 190 millimeters. The chemical composition and mechanical properties of the AA6061-T6 alloy aluminum are presented in Table 1. The handle of the ceramic ball probe was constructed using SKD 11 steel with a head central diameter of 35x35 millimeters and a handle central diameter of 25x25 millimeters. The tooling material used for pressing was a ceramic ball with a central diameter of 8 millimeters, as detailed in Table 2.

Table 1. Chemical Properties of 6061-T6.

Al	Si	Cu	Mn	Mg	Cr	Zn	Ti	Fe
Base	0.4-	0.15-	0.15	0.80-	0.04-	0.25	0.15	0.70
	0.80	0.40	Max	1.20	0.35	Max	Max	Max

Table 2. Mechanical Properties of Ceramic.

Young's modulus (GPa)	Strength (MPa)	Vicker's hardness number
230	700	300

III. BURNISHING EXPERIMENT

aluminum alloy AA6061-T6 workpieces according to specified dimensions, with a central diameter of 22 millimeters and a length of 190 millimeters, as shown in Figure A. Subsequently, take the prepared AA6061-T6 alloy spool and perform shaping using a turning and peeling method. Utilize a D-shaped cutting blade with a cutting speed of 250 meters per minute and a feed rate of 0.3 millimeters per revolution. Turn and peel the surface to achieve a central diameter of 21 millimeters. The turning and peeling process should result in a length of 70 millimeters, as depicted in Figure B. Introduce the prepared workpiece, shaped according to the specified dimensions, into the surface finishing process using a CNC lathe machine (UL-15 Flat Bed). The designated parameters for this process are rotational speeds of 200, 400, and 600 revolutions per minute and movement speeds of 0.15, 0.25, and 0.35 meters per second, as illustrated in Figure 3.



Figure 4. Ball ceramic Burnishing process.

3.1 Mechanical Properties Testing

the mechanical properties testing process, the strength properties of materials are evaluated, typically through destructive testing. The experiments in this test will involve hardness testing and tensile strength testing.

1.Tensile Strength

This is a test of the material's resistance to tensile forces. A sample of the material to be tested is slowly pulled, and the pulling speed can be calculated using Equation 1 with force and constant rate according to the ASTM E8-04 testing standard. The sizes are indicated in the figure 4 point c. The graph shows the relationship between the material's deformation from the initial point of deformation to the point of fracture, as shown in Figure 4 c. The results are recorded to calculate the average value and to plot a graph using the Minitab program.



Figure 5. ASTM E8-04

3.2 Optimization Process

Experimental Design Using Surface Response Analysis and Box-Behnken Design (BBD) with 3 Factors: Spindle Speeds (X1), Feed Rate (X2), and Depth of Burnishing (X3), consisting of a total of 17 experiments, is presented in Figure 5. The factor levels were determined based on relevant research and experimental tool specifications, with three levels: low (-1), medium (0), and high (1), as shown in Table 3. The experimental sequence is provided in Table 4. The analysis of experimental results was conducted using statistical software, including model accuracy verification, decision-making efficiency (R-Square), and variance analysis.

The prediction equation for the tensile force was derived from the regression equation of the tensile force of the workpiece after burnishing, as shown in Equation (1), where Y represents the response value (tensile force). The analysis involved comparing experimental factors such as spindle speed, feed rate, and depth of tool penetration onto the workpiece. The goal was to identify the most suitable factors and use the composite desirability to measure the satisfaction level of the response. The composite desirability value ranges from 0 to 1, with a value of 1 indicating complete satisfaction with the response [6].

Table 3. Parameter of Burnishing process.

Factor	Level		
	-1	0	1
Spindle speeds (X ₁)(RPM)	200	400	600
Feed rate (X ₂) (mm/min)	0.15	0.25	0.35
Depth of cut (X ₃)	0.03	0.06	0.09

Table 4. Experiment of Burnishing.

		Factor of Experimental			Tensile strength (MPa)
Std	Run	Spindle speeds (RPM)	Feed rate (mm/min)	Depth of Burnishing (mm)	
14	1	400(0)	0.25	0.06	364.0
8	2	600(1)	0.25	0.09	366.5
17	3	400(0)	0.25	0.06	362.5
13	4	400(0)	0.25	0.06	362.5
7	5	200(-1)	0.25	0.09	370.0
10	6	400(0)	0.35	0.03	359.0
16	7	400(0)	0.25	0.06	364.0
5	8	200(-1)	0.25	0.03	364.5
1	9	200(-1)	0.15	0.06	363.5
12	10	400(0)	0.35	0.09	361.5
4	11	600(1)	0.35	0.06	362.5
15	12	400(0)	0.25	0.06	369.5
3	13	200(-1)	0.35	0.06	361.5
2	14	600(1)	0.15	0.06	362.5
6	15	600(1)	0.25	0.03	367.0
11	16	400(0)	0.15	0.09	363.0
9	17	400(0)	0.15	0.03	359.5

Table 4 shows the results of the tensile strength test, indicating that the tensile strength falls within the range of 359.0 – 370.0 MPa. The analysis of the relationship between response factors utilized a significant level regression model. The quadratic model was found to be appropriate based on the p-value ($p < 0.05$), lack of fit ($p \geq 0.05$), and the coefficient of determination (R^2), which was high.

Table 5. Response surface regression analysis.

Term	Coef	SE Coef	T-Value	P-Value	VIF
Constant	363.200	0.466	778.78	0.000	
Spindle speeds (rpm)	0.000	0.369	0.00	1.000	1.00
Feed rate (mm/min)	-0.938	0.369	-2.54	0.039	1.00
Depth of Burnishing (mm)	2.188	0.369	5.93	0.001	1.00
Spindle speeds (rpm)*spindle Speeds (rpm)	0.587	0.508	1.16	0.286	1.01
Feed rate (mm/min)*Feed rate (mm/min)	-1.288	0.508	-2.53	0.039	1.01
Depth of Burnishing (mm)*Depth of Burnishing (mm)	3.462	0.508	6.81	0.000	1.01

$$S = 1.04283 \quad R^2 = 94.08\% \quad R^2_{adj} = 86.46\% \quad R^2_{pred} = 31.06\%$$

Table 6. Analysis of the Maximum Tensile Strength Variation of the Workpiece.

Source	DF	Adj SS	Adj MS	F-Value	P-Value
Model	9	120.887	13.4319	12.35	0.002
Linear	3	45.312	15.1042	13.89	0.002
spindle speeds (rpm)	1	0.000	0.0000	0.00	1.000
Feed rate (mm/min)	1	7.031	7.0312	6.47	0.039
Depth of cut (mm)	1	38.281	38.2813	35.20	0.001
Square	3	57.762	19.2542	17.70	0.001
spindle speeds (rpm)*spindle speeds (rpm)	1	1.453	1.4533	1.34	0.286
Feed rate (mm/min)*Feed rate (mm/min)	1	6.980	6.9796	6.42	0.039
Depth of cut (mm)*Depth of cut (mm)	1	50.480	50.4796	46.42	0.000
Interaction	3	17.813	5.9375	5.46	0.030
Error	7	7.613	1.0875		
Lack-of-Fit	3	5.313	1.7708	3.08	0.153
Pure Error	4	2.300	0.5750		
Total	16	128.500			

The results of the analysis of the variance of tensile force at a significance level of 0.05 revealed that the p-value for the interaction term was found to be 0.030, and the squared term had a p-value of 0.001. These values are lower than the specified statistical significance level, indicating that there is a curvature on the surface of the response. It can be inferred that a quadratic model can be used to predict the tensile force from the tensile test. The equation predicting the maximum tensile force of the specimen, based on the coefficients obtained from the analysis of the regression equation shown in Table 3, is represented as Equation 2. When considering the adequacy of the model (Lack-of-Fit) as shown in Table 4, the p-value for Lack-of-Fit was found to be 0.153, which is greater than 0.05. Therefore, the null hypothesis cannot be rejected. It can be stated that the regression model obtained is appropriate, and it can be used to predict the maximum tensile force.

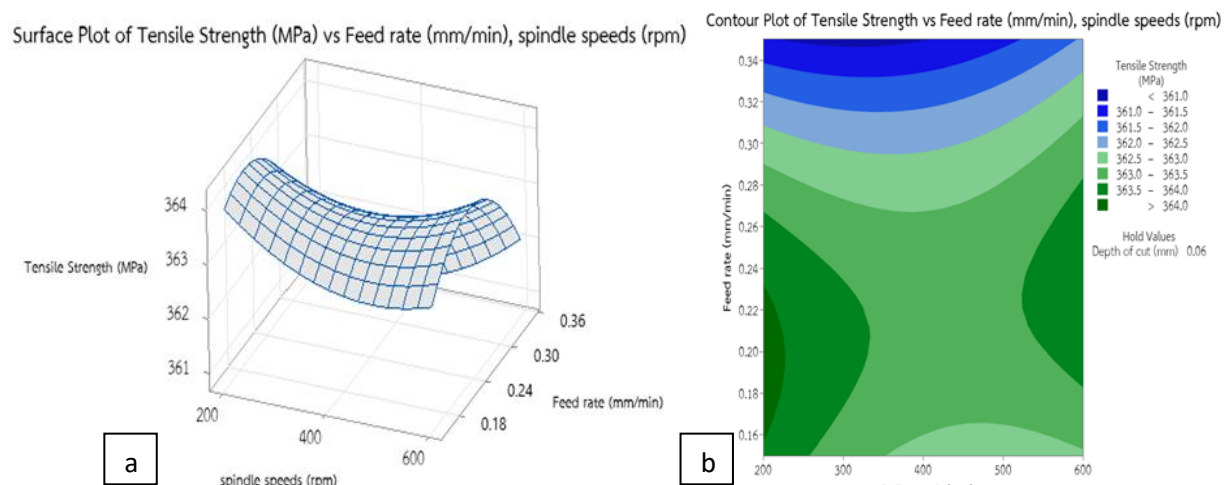


Figure 6. the maximum tensile force of the workpiece (a), surface response (b), and the framework graph between spindle speeds and feed rate.

The response surface for predicting the maximum tensile force value was performed using

the equation obtained for predicting the tensile force value. This surface was then used to generate a response surface graph, as shown in Figure 1, depicting the surface response for the maximum tensile force of the workpiece. In Figure 6(a), the graph illustrates the levels of spindle speeds versus the levels of feed rate. It was observed that when the levels of spindle speeds and feed rate were at intermediate levels, the maximum tensile force value increased and decreased. Subsequently, when the graph showing the combined influence surface between spindle speeds and feed rate, as depicted in Figure 6(a), was presented in the form of a contour plot, the relationship between spindle speeds and feed rate for the amount of tensile force reception was revealed. This relationship exhibited a nonlinear effect, as shown in Figure 6(b). The curved lines in the dark green area indicate significantly higher tensile force reception of the workpiece, exceeding 364.0 MPa. The following curved lines depict the decreasing rates of tensile force reception for the workpiece as 363.5, 363.0, 362.5, and 362.0 MPa, respectively.

the relationship between spindle speed and depth of burnishing, as illustrated in Figure 7. The findings reveal that at moderate levels of spindle speeds, increasing the depth of burnishing results in a decrease in the tensile force of the workpiece, as depicted in Figure 7 (a). Subsequently, the combined influence of spindle speeds and depth of burnishing is presented in a graphical representation. It is evident that the relationship between spindle speeds and depth of burnishing has a non-linear effect on the tensile force, as shown in Figure 7 (b). The bold dark green curve in the central region indicates the maximum tensile force at 370 MPa, while the subsequent curves descending represent reduced tensile forces of 368, 366, and 364 MPa, respectively.

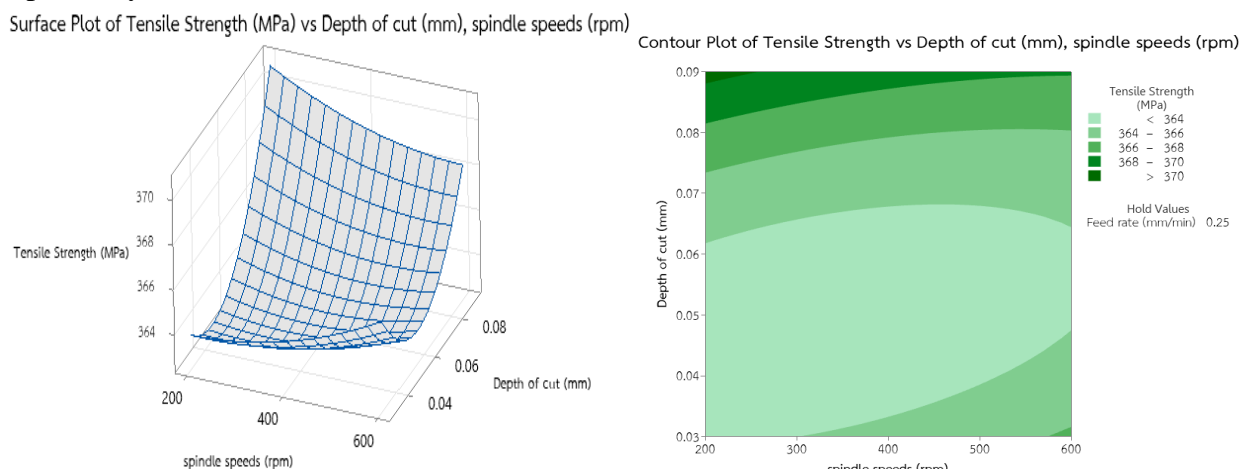


Figure 7. Tensile Strength of the workpiece (a) Surface response (b) Framework graph between Spindle speeds and Depth of Burnishing.

The relationship between the feed rate and the depth of cut affecting the workpiece tensile force was compared. According to Figure 8, it was observed that the tensile force increased when the depth of cut was increased. However, when the depth of cut was decreased, the tensile force was found to decrease, as shown in Figure 8 (a). Subsequently, the influence response surface graph between the feed rate and the depth of cut was presented in a schematic diagram, as shown in Figure 8 (b). It was found that the feed rate and depth of cut did not exhibit a linear relationship. The curved lines in the middle of the graph indicated higher compressive force values exceeding 368 MPa. The subsequent curved lines showed decreasing tensile force values of 366, 364, 362, and 360 MPa.

Surface Plot of Tensile Strength (MPa) vs Depth of cut (mm), Feed rate (mm/min) Contour Plot of Tensile Strength vs Depth of cut (mm), Feed rate (mm/min)

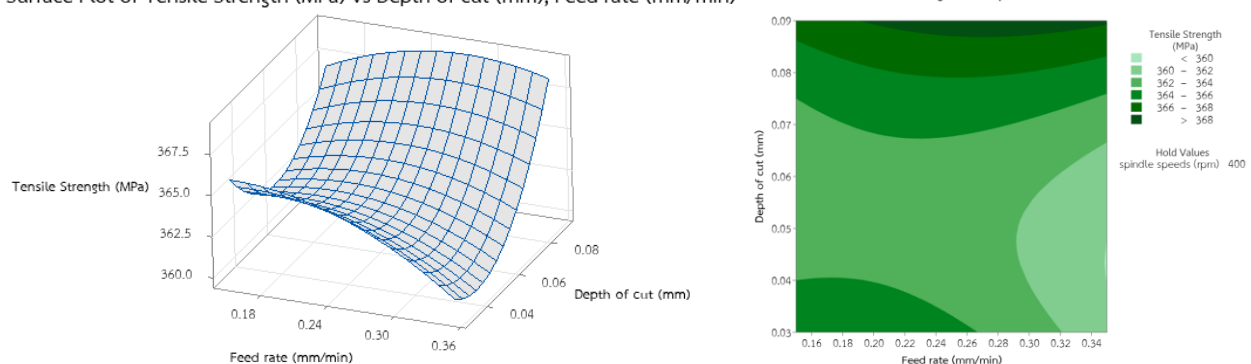


Figure 8. Tensile Strength of the workpiece (a) Surface response (b) Framework graph between Spindle speeds and Depth of Burnishing.

3.3 Experiment Result

The outcomes of the tensile force examination revealed that the tensile force fell within the range of 359.0 – 370.0 MPa. The investigation into the correlation between the response factors employed a regression model at a significance level of $\alpha = 0.05$. The quadratic simulation was deemed appropriate based on the p-value ($p < 0.05$), lack of fit ($p \geq 0.05$), and a high coefficient of determination (R^2). The R^2 values analyzed in Table 5 illustrate the regression analysis. Notably, the R^2 value attains a percentage of 94.08%, signifying that the independent variables (Spindle speeds, Feed rate, and Depth of cut) can elucidate the variation or alteration in the variables. This underscores the model's capacity to formulate a pertinent prediction equation for the response value.

VI. CONCLUSION

This research aims to find suitable parameters in the Burnishing Process on ceramic surfaces with a central hole diameter of 8 millimeters. The specified parameters include cutting speed, feed rate, and depth of feed, with the intention of applying them in the production of various machine components. Test pieces were used to measure hardness, tensile strength, and analyze the microstructure. The study summarized the appropriate parameters and experimental results as follows:

1. Analysis of the factors influencing the tensile strength in the Burnishing Process revealed that the tensile strength ranged from 359.0 to 370.0 MPa. The optimal parameters were found to be a cutting speed of 200 revolutions per minute, a feed rate of 0.2571 meters per minute, and a feed depth of 0.090 millimeters.
2. Analysis of the factors influencing the hardness of the workpiece showed that it ranged from 111.000 to 121.774 Hv. The suitable parameters were determined to be a cutting speed of 393 revolutions per minute, a feed rate of 0.3258 meters per minute, and a feed depth of 0.090 millimeters.

References

[1] Ozer, M., Dalli, K., & Ozer, A. (2023). Effect of ball-burnishing on surface integrity and fatigue behaviour of 7175-T6 AA. *Materials Science and Technology*, 39(2), 248-257.

[2] Saffar, S., & Eslami, H. (2022). Increasing the fatigue life and surface improvement of AL7075 alloy T6 by using ultrasonic ball burnishing process. *International Journal of Surface Science and Engineering*, 16(3), 181-206.

[3] Suriya Prasomthong, & Suriya Namkaew, (April, 2021). Application of Taguchi Method for Burnishing Process of AA5052 Aluminum Alloy by Studying the Optimization of Production Machining Parameters.

[4] H. Yilmaz and R. Sadeler, Effect of ball burnishing treatment on the fatigue behavior of 316L stainless steel operating under anodic and cathodic polarization potentials. *Metallurgical and Materials Transactions A*, 2018, 49(11), 5393-5401..

[5] A. Sova, C. Courbon, F. Valiorgue, J., Rech, and Ph. Bertrand, Effect of turning and ball burnishing on the microstructure and residual stress distribution in stainless steel cold spray deposits. *Journal of Thermal Spray Technology*, 2017, 26(8), 1922-1934.

[6] Raza, A., & Kumar, S. (2022). A critical review of tool design in burnishing process. *Tribology International*, 174, 107717.

[7] Diekmann, James E., & Nelson, Mark C. (1985). Construction Claims: Frequency and Severity. *Journal of Management in Engineering*, 111(1), 74-81.

[8] Ekakul, T. (2000). *Research Methods in Behavioral Science and Social Science*. (8th edition). Chulalongkorn University, Bangkok, Thailand.

[9] K. Hinkelmann and O. Kempthorne, *Design and analysis of experiments, Volume 1: Introduction to experimental design* 1st ED., John Wiley and Sons, Inc., NY, USA, 1994

[10] Prasomthong, S., & Charoenrat, S. (2022). The The optimization of welding hardfacing on wear resistance of FC-25 grey cast iron steel substrate by response surface methodology (RSM). *SNRU Journal of Science and Technology*, 14(2), 245154-245154.

[11] Charoenrat, S., Pookamnerd, Y., & Prasomthong, S. (2021). การพัฒนาสภาพที่เหมาะสมในการเชื่อมพอกผิวต่อการต้านทานการลอกหลุดด้วยกระบวนการเชื่อมแก๊สทั้งสตูนอาร์คแบบลวดร้อนโดยวิธีพื้นผิวดอนสนอง. *The Journal of Industrial Technology*, 17(2), 87-102.

[12] K.Hinkelmann and O. Kempthorne, *Design and analysis of experiments, Volume 1: Introduction to experimental design* 1st ED., John Wiley and Sons, Inc., NY, USA, 1994